structural element i to relate the local axes and a system of multi-global axes.

References

[1] Beaufait, F. W., Rowan, Wm. H., Jr., Hoadley, P. G., and Hackett, R. M., *Computer Methods of Structural Analysis*, Prentice-Hall, Englewood Cliffs, N. J., 1970.

[2] Gere, J. M. and Weaver, Wm., Jr., *Analysis of Framed Structures*, Van Nostrand, Princeton, N. J., 1965.

[3] Rubinstein, M. F., *Structural Systems—Static, Dynamic and Stability*, Prentice-Hall, Englewood Cliffs, N. J., 1970.

Pressure Waves for Flow Induced Acoustic Resonance in Cavities

JOHN B. MILES* AND GEORGE H. WATSON†
University of Missouri, Columbia, Mo.

Introduction

FOR several years, considerable interest has been directed toward understanding separated flow, primarily because of its unavoidable occurrence in many aerodynamic configurations.[1] A particular type of separated flow is herein considered, namely, that caused by cavities in aerodynamic surfaces. As pointed out in a review article,[1] the concern of previous investigators into cavity flow has mainly centered around the effects of such flow on drag and heat transfer during steady flow conditions. The situation related to steady cavity flow is reasonably well understood, subject to certain geometrical constraints.

More recently, it has been observed by several investigators[2–5] that cavities will emit acoustic radiation of a sharply defined frequency under proper conditions of external flow and cavity geometry. Relatedly, resonance is noted to significantly alter the drag[6] and heat transfer[4] characteristics of cavities in comparison to their nonresonating performance. To date, very little experimental data is available which would enable one to clearly define the nature of and the requisite conditions for flow-induced acoustic resonance; nor is there any general theoretical agreement concerning these matters.

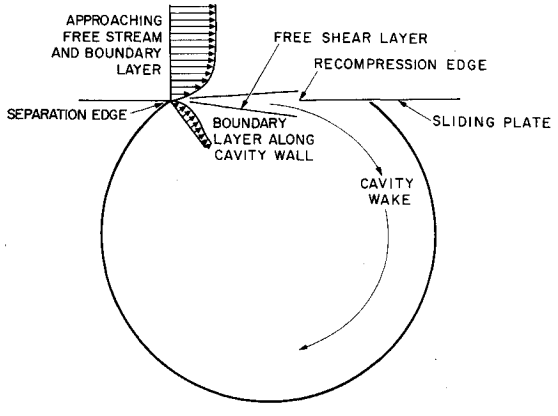

Fig. 1 Cavity flow model.

Received October 26, 1970; revision received February 25, 1971. The subject work was financed in part by University of Missouri Research Council Grant 546.

* Professor, Department of Mechanical and Aerospace Engineering. Member AIAA.

† Former Graduate Student, Department of Mechanical and Aerospace Engineering.

This present Note describes an experimental investigation into the pressure fields existing in cavities during situations of flow-induced resonance, and it represents a portion of a larger study into cavity resonance carried out by coauthor G. H. Watson during his doctoral dissertation.[7] The reported pressure measurements were taken in a near-circular cylinder of 12 in. diam, while the external flow velocity ranged from about 30 to 200 fps. Interpretation of the data allows for classifying each instance of resonance into one of three types. Additionally, all the measured resonant frequencies are correlated by a Strouhal number based on cavity diameter.

Experimental Investigation

The cavity model employed was a circular cylinder of 12 in. diam 12 in. length (normal to the flow), as depicted in Fig. 1. The portion of the cavity adjacent to the freestream was sliced off, resulting in a 9 in. depth and a maximum cavity opening (mixing length) of 8.75 in. The mixing length could be adjusted to any value less than its maximum value by means of the indicated sliding plate, which was constructed from $\frac{1}{16}$-in. steel plate and had a sharpened upstream edge. One end of the cavity model, constructed of $\frac{1}{4}$-in. aluminum plate, had 23 threaded holes located as shown to scale by the crosses in Figs. 2–4. These holes accepted either flush mounted pressure transducers or blank plugs.

The primary flow was through a 1 × 1 ft nozzle exhausting to the atmosphere following an 8:1 contraction. The plate just upstream of the cavity was actually one wall of the nozzle, and it was equipped with a perforated surface which allowed for boundary-layer removal or augmentation. The influence of the condition of the boundary layer at separation will not be herein considered, although Watson[7] did consider it in detail; suffice it to say that thin boundary layers at separation promote both the occurrence and the intensity of resonance.

The existence of flow-induced resonance in the cavity could be ascertained simply by noting the sound generated. More quantitatively, an oscilloscope tracing from one of the aforementioned pressure transducers during a quiescent condition revealed a random pressure fluctuation within the cavity of a relatively small amplitude; conversely, when the cavity was in a resonant condition the pressure variation was distinctly sinusoidal and of a much larger value. The controllable experimental parameters which were found to influence the occurrence of resonance are free-stream velocity, mixing length, and boundary-layer thickness at separation.

The testing procedure developed for the present purposes consisted of setting the boundary-layer control and the mixing length to particular values and then gradually increasing the freestream velocity until a sharply tuned condition of resonance was obtained, as indicated by a pressure transducer output. Then a mapping of the resulting pressure field was obtained by simultaneously monitoring the output from two

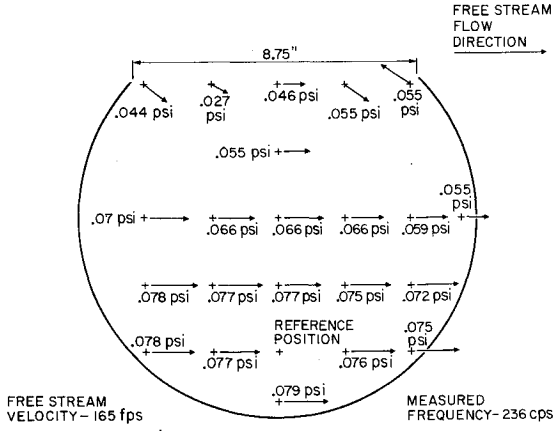

Fig. 2 Polar plot of acoustic pressure within cavity (Helmholtz mode).

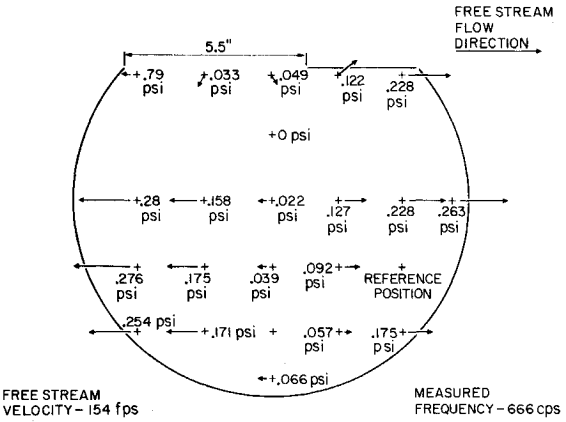

Fig. 3 Polar plot of acoustic pressure within cavity (half-wave mode).

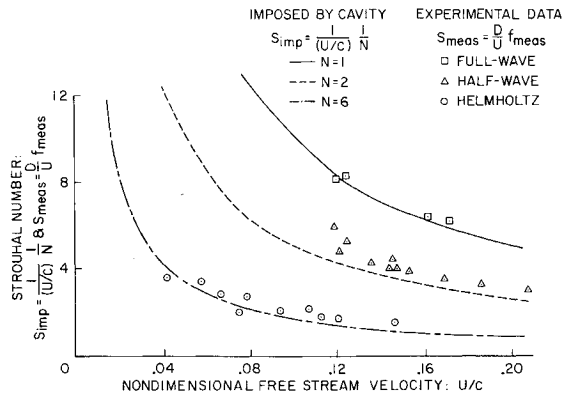

Fig. 5 Strouhal number as function of nondimensional freestream velocity.

pressure transducers. One transducer was fixed in an arbitrarily assigned reference (for relative phase) location, while the other was located progressively in each of the remaining 22 mounting holes. This allowed for presenting information of the type appearing in Figs. 2–4, wherein the length of the arrow at each location represents the magnitude of the measured pressure fluctuation (peak-to-peak) and the direction of the arrow indicates phase angle relative to the arbitrary reference location. For a particular mixing length and boundary-layer condition, the cavity might move in and out of resonance several times as the freestream velocity is increased.

Of special interest in all observed instances of resonance (with the exception of those occurring for very small mixing length) is the fact that all pressure mappings can be classified as one of three types: Helmholtz mode, half-wave mode, or full-wave mode. (It might be noted that these latter two modes correspond approximately to mode number designations of (1, 0, 0) and (2, 0, 0), respectively, according to conventional acoustic theory for standing waves in cavities as presented by Morse and Ingard.[8]) The Helmholtz mode (Fig. 2) is characterized by the pressure fluctuations being in-phase and nearly equal throughout the entire cavity. Cases of the half-wave mode (Fig. 3) feature a standing pressure wave aligned in the direction of the freestream with a pressure node along the vertical diameter and pressure antinodes in both the extreme upstream and downstream regions of the cavity. The full-wave mode likewise had a standing wave aligned with the freestream, but two vertical lines of pressure nodes appear as in Fig. 4. Pressure mappings during resonance occurring with very small mixing lengths revealed that the standing wave was not necessarily aligned with the freestream; this is not surprising when considering that the

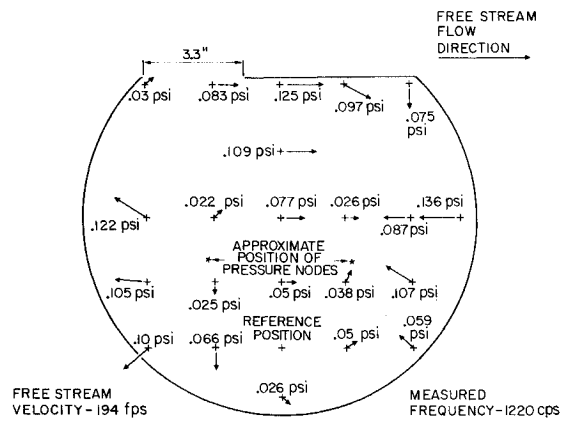

Fig. 4 Polar plot of acoustic pressure within cavity (full-wave mode).

directionality of the freestream must be imparted to the cavity through the mixing length.

Following the lead of other investigators of periodic flow phenomena and guided by the results represented by Figs. 2–4, the measured frequencies for the various observed resonant conditions were computed in a nondimensional manner by employing a Strouhal number based on the cavity diameter. Specifically, each measured resonant frequency (f_{meas}) was converted to a Strouhal number (S_{meas}) by the equation

$$S_{meas} = Df_{meas}/U = Df_{meas}/(U/c)c$$

where D is cavity diameter, U is freestream velocity and c is the speed of sound. For sake of comparison, the frequency imposed (f_{imp}) by the cavity is considered to be:

$$f_{imp} = c/\text{wavelength} = c/ND$$

N represents the number of cavity diameters contained in a resonant wavelength (i.e., $N = 1$ for full-wave mode and 2 for half-wave mode). Converting f_{imp} to an imposed Strouhal number (S_{imp}) gives:

$$S_{imp} = Df_{imp}/U = Dc/UND = 1/(U/c)N$$

The results of this nondimensional consideration are shown in Fig. 5. It is observed that the value $N = 6$ correlates the data for the Helmholtz mode cases quite well. Furthermore, the data from the half-wave events fall slightly above the expected curve of $N = 2$. This is not surprising when considering that the average streamwise dimension of the cavity is somewhat less than the cavity diameter.

Conclusions

From the discussed experimental study, it is concluded that flow induced acoustic resonance in relatively open cavities occurs in one of three modes: Helmholtz, half-wave, and full-wave. During the latter two, a standing pressure wave is aligned with the free stream and its wavelength (consequently frequency) is controlled by the cavity diameter (streamwise dimension). For the Helmholtz case the measured frequencies correspond to wavelengths of 6 times the cavity diameter.

References

[1] Fletcher, L. S., Briggs, D. G., and Page, R. H., "A Review of Heat Transfer in Separated and Reattached Flows," AIAA Paper 70-767, Los Angeles, Calif., 1970.

[2] Krishnamurty, K., "Acoustic Radiation From Two-Dimensional Rectangular Cutouts in Aerodynamic Surfaces," TN 3487, 1955, NACA.

[3] Krishnamurty, K., "Sound Radiation From Surface Cutouts in High Speed Flow," Ph.D. thesis, 1956, California Institute of Technology, Pasadena, Calif.

[4] Miles, J. B., "Stanton Number for Turbulent Flow Past Relatively Deep Cavities," Ph.D. thesis, 1963, Dept. of Mechanical and Industrial Engineering, Univ. of Illinois, Urbana, Ill.

[5] Torda, T. P. and Patel, B. R., "Investigations of Flow in Triangular Cavities," *AIAA Journal*, Vol. 7, No. 12, Dec. 1969, pp 2365-2367.

[6] McGregor, O. W., "Aerodynamic Drag of Two-Dimensional Rectangular Notches in Transonic and Supersonic Turbulent Flow (With Emphasis on the Effects of Self-Induced Pressure Oscillations)," Ph.D. thesis, 1969, Dept. of Mechanical and Industrial Engineering, Univ. of Illinois, Urbana, Ill.

[7] Watson, G. H., "An Analysis of Flow Induced Acoustic Resonance in Cavities," Ph.D. thesis, 1970, Dept. of Mechanical and Aerospace Engineering, Univ. of Missouri, Columbia, Mo.

[8] Morse, P. M. and Ingard, K. U., *Theoretical Acoustics*, McGraw-Hill, New York, 1968, Chap. 9.

Electrostatic Probe Electron Current Collection in the Transition Regime

E. W. PETERSON*
University of Minnesota, Minneapolis, Minn.

Introduction

TALBOT and Chou[1] recently developed an approximate analytical analysis, based on the limited results of the rigorous Chou-Talbot-Willis[2] theory, which permits the calculation of the effect of collisions on the probe ion or electron current in the electron retarding field region. Their analytical results have been found to compare favorably with the Kaegi-Chin[3] and Dunn-Lordi[4] ion current measurements and with the Kirchhoff-Peterson-Talbot[5] ion and electron current measurements, all taken using negatively biased cylindrical probes operating in the transition regime. However, the influence of collisions on the electron current attracted to a positively biased probe is also of practical interest. It is therefore the intent of this work to extend the Talbot-Chou[1] approximate analysis to describe the influence of collisions on the electron current collected by a positively biased cylindrical or spherical probe.

In the Chou-Talbot-Willis[2] collisional analysis certain integrals appeared which, because of their complexity, were only evaluated over a small range of the parameters of interest in order to establish the trend of the results. However the applications of these results for negatively biased probes were extended by Talbot and Chou[1] to include the entire range of parameters. This was accomplished by using the Bernstein-Rabinowitz[6] and Laframboise[7] results and the Su-Lam[8] and Cohen[9] results to evaluate these integrals in the collisionless and continuum limits respectively and then using an interpolation formula to span the transition regime between these limits. The same general procedure may be followed for positively biased probes.

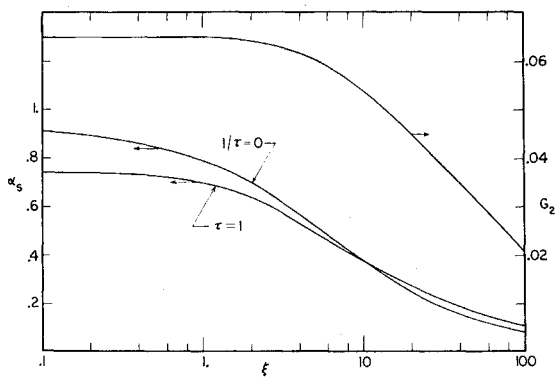

Fig. 1 Functions for evaluation of spherical probe current.

One can show that the *rigorous* analytical expressions needed to evaluate the collisionless limits of these integrals for positive probe potentials may be obtained from the Talbot-Chou[1] results for negative probes by interchanging (the notation is that of Ref. 1) n_e and n_i, j_e and j_i and by everywhere replacing $\tau\chi$ by $(-\chi)$ and χ by $(-\tau\chi)$. Similarly the *rigorous* equations for the positive probe valid in the continuum limit may be recovered by interchanging j_e and j_i; K_e and K_i, ξ_e and ξ_i, and by everywhere replacing τ by $1/\tau$. However certain algebraic approximations are also used in the evaluations of these integrals and the resulting probe currents. Obviously the analogous expressions for the positive probe can not be determined by direct substitution from the negative probe results of Talbot and Chou[1] and will therefore be discusssed in detail in the following paragraphs.

Spherical Probe

First consider the spherical case where for positive probe potentials the integral is of the form $J = \int_0^1 \exp(\chi)dz$. In order to evaluate the potential distribution $\chi(z)$ in the collisionless limit it is necessary to have an algebraic representation for the probe current ($j_{e,\infty}$). To be consistent, an expression similar in form to that used for ion current in Ref. 1 is desired. Fortunately Laframboise's[7] numerical results for monoenergetic electrons can be represented within 5% by

$$j_{e,\infty} = f_s(\tau)(\chi_p/\tau\chi_s)\alpha_s \tag{1}$$

provided $f_s(\tau)$ is defined as

$$f_s(\tau) \equiv 1 - \pi\chi_s/4 = j_{e,\infty}z_s^2 \tag{2}$$

Representative values of f_s, $\tau\chi_s$ are shown on Table 1 while α_s is given on Fig. 1. It follows that the potential distribution, which must vary continuously throughout the region $z_s \leq z \leq 1$ and must satisfy Eqs. (1) and (2) at the probe and absorption radii, respectively, may be approximated by

$$j_{e,\infty}z^2 = f_s(\tau)(\chi/\chi_s)^{\beta_s} \tag{3}$$

where

$$\beta_s = \alpha_s[1 - \ln\tau/\ln(\chi_p/\chi_s)] \tag{4}$$

The above integral may then be numerically evaluated. For electron collection the contribution from the outer integral (over the region $0 \leq z \leq z_s$) is of the form $J_{e,\infty}^{(1)} = G_1(\tau)/j_{e,\infty}^{1/2}$ while the inner integral ($z_s \leq z \leq 1$) may be taken, with only a small loss in accuracy, as $J_{e,\infty}^{(2)} = \tau^{1/2}G_2(\xi)$. Representative values of G_1 and G_2 are given in Table 1 and Fig. 1 respectively. For monoenergetic ion collection the integral analogous to $J_{e,\infty}^{(2)}$ is negligible. However, recall that the amount of electric field that penetrates past the sheath edge is nearly proportional to the thermal energy of the repelled species. Therefore for large τ the ion shielding at positive probe potentials is nearly complete and the contribution from the inner integral may equal that from the outer. It follows that the electron current attracted to a spherical probe operating in the transition regime is given by,

$$j_{e,\infty}/j_e = 1 + (1 + K_e)^{-1}[G_1(\tau)j_{e,\infty}^{1/2} + \tau^{1/2}j_{e,\infty}G_2(\xi)] + K_e^{-1}(1 + K_e)^{-1}(1 + \tau^{-1})^{-1}j_{e,\infty}z_0 \tag{5}$$

Table 1 Functions for the evaluation of the probe current

	$\tau = 1$	$\tau = 2$	$\tau = 5$	$\tau = 10$
$-\tau\chi_s$	0.52	0.59	0.65	0.67
$f_s(\tau)$	1.41	1.23	1.10	1.06
$G_1(\tau)$	1.07	1.05	1.03	1.02
$f_c(\tau)$	1.38	1.20	1.08	1.04

Received June 10, 1970; revision received January 18, 1971.
* Assistant Professor. Member AIAA.